Quantifying the economic value of 2nd-life electric vehicle batteries used for stationary applications

December 12, 2019

Richard Li and Sara Borchers

ABSTRACT

The expected strong increase in electric vehicle (EV) adoption will result in the availability of terawatt-hours of batteries that no longer meet the standards for usage in EVs (Engel 2019). EV performance standards for Li-ion batteries typically include maintaining 80% of their initial capacity. Once these standards are no longer satisfied, these batteries can be redeployed into a secondary market, introducing additional services and revenue, and minimizing resource extraction for battery production. However, since the market for second-life batteries is relatively nascent, little research has been done to predict how these batteries will perform. This paper presents a model for calculating battery degradation as a function of capacity fade and resistance growth. It is applied to second-life batteries used in two stationary applications: frequency regulation and fast charging. The results indicated that there is a tradeoff between battery sizing and cell lifetime. Oversizing the battery system allows cells to operate at a lower depth of discharge, which extends battery life – however, this requires more batteries to serve the same application. In the case of frequency regulation, the greatest lifetime value ($2355) was generated at a 10% depth of discharge. In the case of fast-charging support, the greatest lifetime value ($148) was generated at a 50% depth of discharge. It is important to note that the economic value can vary widely, due to differences in compensation rates across the country.

INTRODUCTION

The development of second-life applications for electric vehicle (EV) Li-ion batteries has significant environmental impact. The global EV stock is projected to exceed 130 million by 2030 (IEA 2019). This significant ramp-up of Li-ion production will place a strain on the global supply of cobalt and nickel. Additionally, lithium production requires high levels of water, and often takes place in drought-ridden regions. Battery reuse would reduce the rate of primary resource extraction.

Second-life applications also have the potential to improve the economics of the EV market. The price premium of EVs is still the #1 concern among American consumers (Woodward 2019). Since the battery makes up 33% of the retail cost of an EV (Bullard 2019), second-life applications that generate additional revenue streams for batteries may lower the upfront cost of EVs, thereby driving widespread adoption of EVs.

Navigant Research predicts that the global second-life battery business will grow from $16 million in 2014 to $3 billion in 2035. Consequently, research into second-life opportunities has sky-rocketed in recent years. For instance, U.S. Department of Energy's Vehicle Technologies Office funded the National Renewable Energy Laboratory (NREL) to investigate the feasibility and major barriers to adoption of second-life Li-ion batteries. NREL found that battery degradation in both first and second-life is a "critical uncertainty" in the feasibility analysis. Repurposing can only be successful if the second-life battery is reliable. Our model seeks to address this barrier by predicting degradation of Li-ion batteries in second-life applications.

METHODOLOGY

First, we reconstructed the battery degradation model developed by NREL (Smith et al. 2017). To construct this model, aging tests were conducted on 75-Ah Kokam NMC cells. A general lifetime prognostic model framework was applied to model changes in capacity and resistance as the batteries were cycled.

Capacity (Q) was taken to be the minimum of Li-limited capacity (Q_{Li}), negative electrode-site-limited capacity (Q_{neg}), or positive electrode-site-limited capacity (Q_{pos}). These three capacities are modeled as follows:

$$Q_{Li} = d_0 \left[b_0 - \underbrace{b_1 t^{1/2}}_{\substack{SEI\ growth \\ with\ calendar \\ time}} - \underbrace{b_2 N}_{\substack{Loss\ with \\ cycling}} - \underbrace{b_3 \left(1 - \exp(-t/\tau_{b3})\right)}_{\substack{Break-in\ mechanism \\ at\ BOL}} \right]$$

$$Q_{neg} = \left[c_0^{\,2} - 2 c_2 c_0 N \right]^{\frac{1}{2}}$$

$$Q_{pos} = d_0 + \underbrace{d_3 \left(1 - \exp(-Ah_{dis}/228)\right)}_{Increase\ in\ capacity\ at\ BOL}$$

The resistance is modeled at 50% SOC as follows:

$$R = \underbrace{R_0}_{\substack{Instantaneous \\ temperature \\ response}} \left[\underbrace{a_0}_{\substack{Base \\ resistance}} + \underbrace{a_1 t^{1/2}}_{\substack{SEI\ growth \\ with\ calendar \\ time}} + \underbrace{a_2 / Q_{neg}}_{\substack{Loss\ with \\ cycling\ (using \\ negative\ site \\ loss\ model)}} - \underbrace{a_3 \left(1 - \exp(-t/\tau_{a3})\right)}_{\substack{Break-in\ mechanism \\ at\ BOL}} + \underbrace{a_4 t}_{\substack{Secondary \\ calendar\ life \\ term\ proportional \\ to\ time}} \right].$$

Once this initial model was recreated, we adjusted the battery inputs to reflect second-life battery conditions. We increased the starting resistance by 25%. This value was chosen based on the resistance growth demonstrated in a new battery after 1,000 cycles at 80% DOD. We decreased the starting capacity by 20%, since most EV manufacturers mark this capacity fade as the end of life (Saxena 2015). Lastly, we removed break-in mechanisms (b_3 and a_3 terms in capacity and resistance models, respectively), since these mechanisms would no longer be active during the second life.

Next, we constructed SOC curves that simulate our stationary applications. For the frequency regulation application, the frequency signal was collected from one day of PJM frequency regulation data (PJM 2019). As a first approximation, the frequency signal was directly scaled into a SOC curve, i.e. frequencies of (–1, +1) mapped to SOCs of (0.45, 0.55), for 10% DOD.

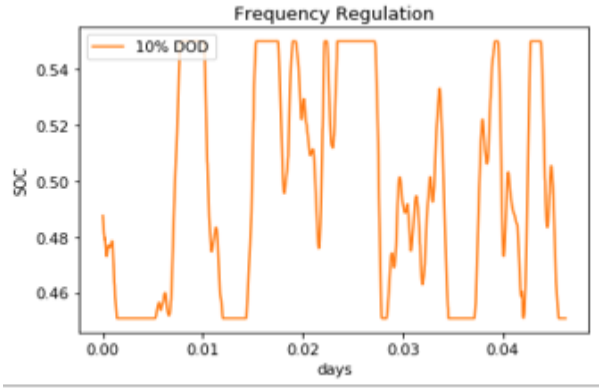

Figure 1. *State-of-charge profile for battery used for frequency regulation at 10% depth-of-discharge, over 1 hour.*

For the fast charging application, the shape of the SOC curve was based on a discharge rate of 3C, and recharge rate at 1C. We estimated that a single fast charger will be used 12 times per day. Varying DODs were inputted to determine their effect on lifetime. To construct an SOC curve, we first calculated the number of minutes needed for a charging and discharging using the following formula:

$$minutes = \frac{(Ah_{initial} - Ah_{final}) * (\frac{1}{C - rate})}{Ah} * 60$$

For a used Kokam cell, $Ah_{initial}$ is 75Ah * 0.8 = 60Ah. Ah_{final} is determined by the DOD. Once the minutes for a charging and discharging session were calculated, the slope of the SOC curve for the charge and discharge was calculated as ΔSOC/minutes. With the slope of the curve and the initial and final SOC values (determined by the DOD), a complete SOC curve was constructed:

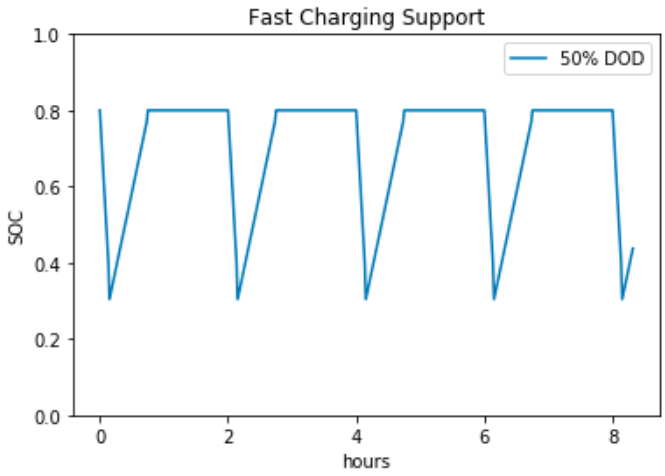

Figure 2. *State-of-charge profile for battery used for fast-charging at 50% depth-of-discharge, over 8 hours.*

We ran the model with the adjusted battery inputs and SOC curves to determine the end of life. The end of life was defined as the point at which the battery can no longer serve its function because capacity is too low for the necessary DOD, or resistance is too high for the necessary current.

Finally, we calculated the economic value of a cell generated over its second-life lifespan. We used PJM regulation market rates, but it is important to note that compensation schemes vary widely across the country. We normalized the value generated on a per-cell basis to compare across different applications without needing to explicitly calculate the cost of a second-life cell, since the second-life battery market is still very nascent and costs of batteries are not standardized.

RESULTS

Frequency Regulation:

The SOC profile for FR is characterized by rapid, irregular cycles (115 cycles/day). We modeled the degradation of the battery at 3 different maximum DODs: 30%, 20%, and 10%.

The end of life was defined as the point at which the battery capacity fades to twice the capacity that it discharges at the beginning of second life. For instance, a 60Ah battery at 10% DOD would discharge 6Ah in the beginning of its second life. Its end of life is reached when its capacity fades to 12Ah.

With a maximum DOD of 30%, the capacity of the battery faded to 48Ah in 2.1 years. With a maximum DOD of 20%, the capacity of the battery faded to 24Ah in 5.0 years. With a maximum DOD of 10%, the capacity of the battery faded to 12Ah in 12.2 years.

Over the lifespan of these batteries, the resistance increases by up to 3x, but this should not be an issue for frequency regulation, as it does not require high power outputs to function. As a result, these batteries are capacity-limited and not resistance-limited.

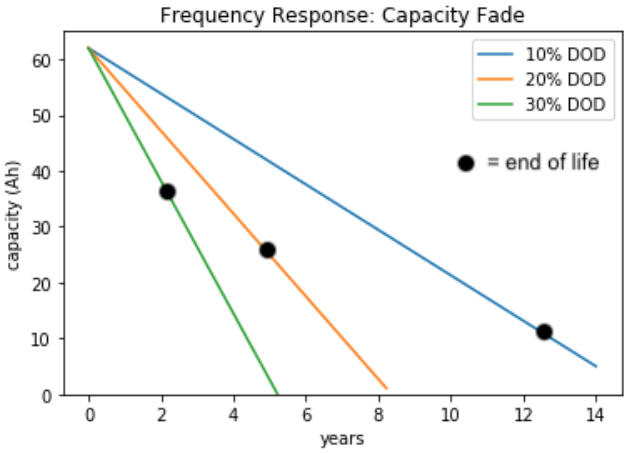

Figure 3. *Capacity fade at different DODs in second-life batteries used for frequency regulation.*

Fast Charging Support

The SOC cycle for fast charging support is characterized by slower, deeper cycles (12 cycles/day). We modeled the degradation of the battery at 4 different maximum DODs: 10%, 30%, 50%, and 70%.

The end of life was defined as when the resistance doubles, at which point power output (3C) is halved (1.5C) and can no longer provide fast charging. This occurs from 0.9–7.7 years, depending on the depth of discharge.

At the point where batteries become resistance limited, they still have sufficient capacity to perform their initial depth of discharge. For example, the cell discharged at 30% DOD (18 Ah) becomes resistance-limited at 6.3 years, at which point the capacity is still 30 Ah. This suggests the cells in this application are resistance-limited, not capacity-limited.

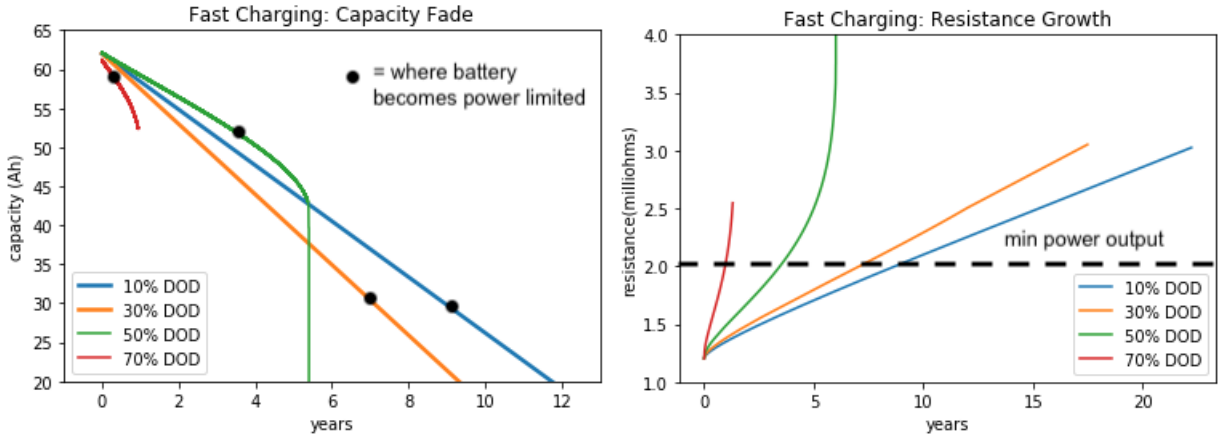

Figure 3. *Resistance growth and capacity fade at different DODs in second-life batteries used for fast-charging.*

The graphs for 50% and 70% DOD abruptly end where the battery capacity is no longer sufficient to perform the required depth of discharge. At this point, the DOD parameter in the model exceeds 100% and causes abnormal model behavior.

Economic Value

For each application, we calculate the economic value generated by a single cell under different system sizing scenarios.

The value for frequency regulation was calculated by multiplying the 2017 PJM price of frequency regulation by the total MWh discharged by a single cell over its lifespan. For instance, for the 10% DOD case:

$$\left(\frac{\$0.21}{MWh}\right)\left(115\,\frac{cycles}{day}\right)(12.2\,yrs)\left(\frac{365\,days}{1\,yr}\right)\left(\frac{0.1\,SOC}{1\,cycle}\right)\left(\frac{60\,Ah}{1\,SOC}\right)(3.65V)\left(\frac{1\,MWh}{1000Wh}\right)=\$2355$$

The value for fast charging support was calculated by first sizing the battery system that would be needed for the application. We scale our battery system to provide half of the power to fast charge one 66 kWh EV, to mitigate demand charges. First, we find the number of batteries required to provide 33 kWh of energy. In this example, we used a DOD of 50%:

$$(1/2)\frac{66kWh(\frac{1000W}{1kW})}{(60Ah)(0.5DOD)(3.65V)}=301\,batteries$$

Next, we ensure that this number of batteries is sufficient to provide half of the power needed for a fast charge. The minimum rate of fast charging is 1.5 C. We will discharge our second-life battery up to 1.5 C:

$$(1/2)(66kWh)(1.5C) \leq (301\,batteries)(60\frac{Ah}{battery})(1.5C)(3.65V)(\frac{1kW}{1000W})$$

$$49.5kWh \leq 98.4kWh$$

Thus, our battery system is sufficiently sized to provide half of the power of the fast charge at this DOD.

The value generated by this battery system for fast charging can be calculated as follows, using a demand charge tariff of $15/kW (2017 NREL survey):

$$\frac{\$30}{(kW)(billing\,cycle)}(33kW)(\frac{12\,billing\,cycles}{year})(3.11years) = \$36940$$

Lastly, we normalize by a per-cell basis:

$$\frac{\$36940}{301\,batteries} = \frac{\$122}{battery}$$

When we performed these calculations for all applications and DOD variations, we found that there is a tradeoff between battery sizing and cell lifetime. Oversizing the battery system allows cells to operate at a lower depth of discharge, which extends battery life – however, this requires more batteries to serve the same application.

FREQ RESPONSE	**10% DOD**	**20% DOD**	**30% DOD**
Lifetime (years)	12.2	5.0	2.1
Value generated over cell lifetime	$2355	$1930	$1216

FAST CHARGING	**10% DOD**	**30% DOD**	**50% DOD**	**70% DOD**
Lifetime (years)	7.7	6.3	3.1	0.9
Batteries required	1505	502	301	215
Value generated over cell lifetime	$61	$148	$122	$47

CONCLUSION

Key Takeaways

Second-life batteries appear to generate significantly more value in frequency response applications compared to fast charging support, although these economic calculations are sensitive to significant market fluctuations. For instance, the demand charges we used ($30/kW) are considered average for California according to the 2017 NREL survey, but can be range from $15-100 depending on time of day and season. Further, a more sophisticated model would optimize

for the configuration of cells in series and parallel to provide exactly the power and energy required for the fast charging application.

Within an application, there is a tradeoff between battery sizing and cell lifetime. Oversizing the battery system allows operation at a lower depth of discharge, extending battery life – but requires more batteries. This appears to be the driving force in frequency response, as these cells are cycled rapidly, and thus depth of discharge must be minimized.

For fast charging, which is resistance-limited, the benefits of oversizing the system become outweighed by the increasing number of batteries required. Thus, 30% DOD optimizes this tradeoff of battery deterioration vs. battery performance.

Future Work

To refine this model, internal temperature should fluctuate as the battery cycles. Currently, we are assuming thermal management and keeping internal temperature constant. However, even with thermal controls, the internal temperature of a battery will rise during the constant current stage of discharge, and fall during the constant voltage stage of the charge.

We attempted to program these fluctuations into our model, but found that since resistance is highly dependent on temperature, this model outputted resistance curves with extreme fluctuations, making it difficult to see meaningful growth over the lifespan of the battery. To properly model internal temperature, it should be calculated as a function of current and resistance at each point in time.

It would also be interesting to compare degradation across a wider variety of stationary applications, such as self-consumption. Tesla is currently creating battery packs for EVs and self-consumption, and using the same cells for both. This particular case is well-suited for second-life batteries, since both devices are already designed around the same battery technology. Modeling the lifespan of a second-life EV battery in a Powerpack and comparing it to a new battery could inform decisions about when second-life installations make economic sense.

ACKNOWLEDGEMENTS

We would like to thank Robert Tietje (VW) for his insight on EV 2nd life opportunities, Melanie Senn (VW) for her advice on modeling battery degradation, and Kandler Smith (NREL) for his guidance in adapting the NREL BLAST model.

Special thanks to Dr. Ram Rajagopal, Dr. Abbas El Gamal, and Thomas Navidi for their support in our project development.

REFERENCES

NREL. “Battery Second Use for Plug-In Electric Vehicles.” n.d. Accessed December 1, 2019. https://www.nrel.gov/transportation/battery-second-use.html.

Bloomberg.Com. 2019. “Electric Car Price Tag Shrinks Along With Battery Cost,” April 12, 2019. https://www.bloomberg.com/opinion/articles/2019-04-12/electric-vehicle-battery-shrinks-and-so-does-the-total-cost.

Casals, Lluc Canals, B. Amante García, and Camille Canal. 2019. “Second Life Batteries Lifespan: Rest of Useful Life and Environmental Analysis.” *Journal of Environmental Management* 232 (February): 354–63. https://doi.org/10.1016/j.jenvman.2018.11.046.

Woodward, Mike. “New markets. New entrants. New Challenges.” Deloitte. 2019. https://www2.deloitte.com/content/dam/Deloitte/uk/Documents/manufacturing/deloitte-uk-battery-electric-vehicles.pdf.

Engel, Hauke, Hertzke, Patrick, and Siccardo, Giulia. “Second life EV batteries: The newest value pool in energy storage.” McKinsey and Company. April 2019. https://www.mckinsey.com/industries/automotive-and-assembly/our-insights/second-life-ev-batteries-the-newest-value-pool-in-energy-storage.

IEA (2019), "Global EV Outlook 2019", IEA, Paris https://www.iea.org/reports/global-ev-outlook-2019

Neubauer, Jeremy S., Eric Wood, and Ahmad Pesaran. 2015. “A Second Life for Electric Vehicle Batteries: Answering Questions on Battery Degradation and Value.” *SAE International Journal of Materials and Manufacturing* 8 (2): 544–53. https://doi.org/10.4271/2015-01-1306.

Novais, Susana, Micael Nascimento, Lorenzo Grande, Maria Fátima Domingues, Paulo Antunes, Nélia Alberto, Cátia Leitão, et al. 2016. “Internal and External Temperature Monitoring of a Li-Ion Battery with Fiber Bragg Grating Sensors.” *Sensors (Basel, Switzerland)* 16 (9). https://doi.org/10.3390/s16091394.

“PJM - Ancillary Services.” n.d. Accessed November 12, 2019. https://www.pjm.com/markets-and-operations/ancillary-services.aspx.

Saxena, Samveg, Caroline Le Floch, Jason MacDonald, and Scott Moura. 2015. “Quantifying EV Battery End-of-Life through Analysis of Travel Needs with Vehicle Powertrain Models.” *Journal of Power Sources* 282 (May): 265–76. https://doi.org/10.1016/j.jpowsour.2015.01.072.

Smith, Kandler, Aron Saxon, Matthew Keyser, Blake Lundstrom, Ziwei Cao, and Albert Roc. 2017a. “Life Prediction Model for Grid-Connected Li-Ion Battery Energy Storage System.” In *2017 American Control Conference (ACC)*, 4062–68. Seattle, WA, USA: IEEE. https://doi.org/10.23919/ACC.2017.7963578.